Supplementary Materials for

Single Reconstituted Neuronal SNARE Complexes Zipper in Three Distinct Stages

Ying Gao, Sylvain Zorman, Gregory Gundersen, Zhiqun Xi, Lu Ma, George Sirinakis, James E. Rothman*, Yongli Zhang*

*Correspondence to: yongli.zhang@yale.edu and james.rothman@yale.edu

This PDF file includes:

Materials and Methods

SNARE proteins and peptide

The synaptic SNARE complex consists of VAMP2 (synaptobrevin), syntaxin 1, and SNAP-25 (*1*). VAMP2 is inserted into the synaptic vesicle membrane by a C-terminal trans-membrane anchor (*33*), and contributes one helix to the bundle. Syntaxin 1 is inserted into the plasma membrane similarly (*34*), and contributes a second helix. SNAP-25 is attached to the plasma membrane only by fatty acylation (*35*), and contributes the final two helices. When fully assembled, as after fusion is complete, the cytoplasmic portion of SNARE complex has a tripartite anatomy. The four helix bundle contains 15 hydrophobic heptad repeat layers in its core. The bundle is divided approximately evenly into an N-terminal domain (NTD) and a C-terminal domain (CTD) by an exceptional central "ionic layer" consisting of an arginine (R56 in VAMP2) and three glutamine residues in each of the other three helices (Fig. 1A). The corresponding VAMP2 portions in NTD and CTD are referred as "Vn" and "Vc", respectively. VAMP2 and syntaxin continue beyond the four helix bundle as a two-helix bundle to their trans-membrane domains through short "linker" domains (LD). The linker domain of VAMP2 contains residues 85-94 (*16*).

The sequences of syntaxin 1A from rat and of VAMP2 and SNAP-25B from mouse were used in this work. The amino acid sequences of the truncated syntaxin and VAMP2 and the full-length SNAP-25 are listed below.

Constructs for *C*-terminal *p*ulling (CP):

Syntaxin (187-265)

190 200 210 220 230 240
SCGGISK*Q*ALSEIETRH*S*EIIKLENSI*R*ELHDMFMDM*A*MLVES**Q**GEM*I*DRIEYNVEH*A*

250 260
VDYVERAVS*D*TKKAV**K**YQS*K*ARRKKGGSGNGGSGS**GLNDIFEAQKIEWHE**DYKD
DDDK

VAMP2 (25-92)

30 40 50 60 70
SCGGSGGNLTSN*R*RLQQTQAQV*D*EVVDIMRVN*V*DKVLE**R**DQK*L*SELDDRADA*L*QA

80 90
GASQFETSAAKLKRKYW*W*KNGGSGNGSGGLCTPSRGGDYKDDDDK

Syntaxin (172-265)
SCGGGNPAIFASGIIMDSSISKQALSEIETRHSEIIKLENSIRELHDMFMDMAMLVES**Q**
GEMIDRIEYNVEHAVDYVERAVSDTKKAVKYQSKARRKKGGSGNGGSGS**GLNDIF
EAQKIEWHE**DYKDDDDK

VAMP2 (1-92)
SCGGMSATAATVPPAAPAGEGGPPAPPPNLTSNRRLQQTQAQVDEVVDIMRVNVDK
VLERDQKLSELDDRADALQAGASQFETSAAKLKRKYWWKNGGSGNGSGGLCTPSR
GGDYKDDDDK

VAMP2 (1-84)
SCGGMSATAATVPPAAPAGEGGPPAPPPNLTSNRRLQQTQAQVDEVVDIMRVNVDK
VLERDQKLSELDDRADALQAGASQFETSAAKLGGSGNGSGGLCTPSRGGDYKDDD
DK

VAMP2 (1-77)
SCGGMSATAATVPPAAPAGEGGPPAPPPNLTSNRRLQQTQAQVDEVVDIMRVNVDK
VLERDQKLSELDDRADALQAGASQFGGSGNGSGGLCTPSRGGDYKDDDDK

Constructs for *N*-terminal *p*ulling (NP):

Syntaxin (172-255)
S**GLNDIFEAQKIEWHE**GGNGGSSGGGNPAIFASGIIMDSSISKQALSEIETRHSEIIKL
ENSIRELHDMFMDMAMLVESQGEMIDRIEYNVEHAVDYVERAVSDTKKAVGSCG

VAMP2 (1-85)
SCGSGNGSGGMSATAATVPPAAPAGEGGPPAPPPNLTSNRRLQQTQAQVDEVVDIM
RVNVDKVLERDQKLSELDDRADALQAGASQFETSAAKLKGSGCG

SNAP-25B (1-206)
MAEDADMRNELEEMQRRADQLADESLESTRRMLQLVEESKDAGIRTLVMLDEQGEQL
ERIEEGMDQINKDMKEAEKNLTDLGKF*S*GL*S*V*S*P*S*NKLKSSDAYKKAWGNNQDGVVAS
QPARVVDEREQMAISGGFIRRVTNDARENEMDENLEQVSGIIGNLRHMALDMGNEIDT
QNRQIDRIMEKADSNKTRIDEANQRATKMLGSG

The original SNARE protein sequences are underlined. Numbering for the wild-type amino acids are indicated above the first two sequences, with the corresponding amino acids in italic. The amino acids in the ionic layer of the four-helix bundle and the linker domain are highlighted in cyan and green, respectively. Other sequences not underlined are added to facilitate attachment of the proteins to the DNA handle, the bead surface, or other SNARE proteins. The Avi-tag sequences are shown in bold and the cysteine residues used for crosslinking are highlighted in red. Syntaxin (187-265) and VAMP2 (25-92) were used to make the SNARE complex containing a *s*hort N-terminal loop for *C*-terminal *p*ulling (SCP), whereas syntaxin (172-265) and VAMP2 (1-92) were utilized in the complex containing a long N-terminal loop for C-terminal pulling (LCP). SCP sequences were used in the experiments related to Figs. 1, 2, S2, S3, S5, S7, S9, and S12. NP sequences were used in Fig. 3, and LCP sequences in figs. S4 and S12. VAMP2 (1-84) and VAMP2 (1-77) were used with syntaxin (172-265) and SNAP-25B to generate the SNARE complex with the truncated linker domain (fig. S6) and the Vc domain (fig. S8), respectively. The protein sequences for C-terminal pulling have C-terminal aldehyde tags (LCTPSR) (*36*) and/or FLAG tags (DYKDDDDK). These tags are designed as alternative tags for DNA handle crosslinking or protein purification, respectively, but are not used in this work. All cysteine amino acids in SNAP-25 were replaced by serine (shown in italic).

Protein purification

Genes corresponding to syntaxin and VAMP2 were inserted into pET-SUMO vectors through TA-cloning. The proteins were then expressed in *E. coli* BL21(DE3) cells and purified as described in the manual of Champion™ pET SUMO Expression System (Invitrogen). Typically, *E.coli* cell pellets were re-suspended in 50mM HEPES, 400 KCl, 10% Glycerol, 10mM imidazole, pH 7.7 and passed through the cell homogenizer three times to obtain clear cell lysates. The lysates were then cleared by ultracentrifugation. The SNARE proteins in the supernatant were bound to Ni-NTA resin and washed by increasing imidazole concentrations up to 20mM. The syntaxin protein was biotinylated in vitro by biotin ligase enzyme (BirA) as described (Avidity, CO). Finally, the His-SUMO tags on both proteins were cleaved directly on Ni-NTA resin by incubating the tagged SNARE proteins/resin slurry with SUMO protease (with a protein-to-protease mass ratio of 100:1) at 4 ˚C overnight. The SNARE proteins were collected in the flow-through while the His-SUMO tag was retained on the resin. SNAP-25 was expressed from the pET-28a vector and purified through its N-terminal His-tag. All SNARE proteins were purified in the presence of 2 mM TCEP to avoid unwanted crosslinking.

Ternary SNARE complex formation and crosslinking

Ternary SNARE complexes were formed by mixing syntaxin, SNAP-25 and VAMP2 proteins with 0.8:1:1.2 molar ratios in 50 mM HEPES, 100 KCl, 5mM TCEP, pH 7.7 and incubating the mixture at 4 °C overnight. Formation of the ternary complex was confirmed by SDS polyacrylamide gel electrophoresis (Fig. S1). Excess SNARE monomers or binary complexes were removed from the ternary complex by gel filtration through Superdex 75 5/150 GL column or by further purification through Ni-NTA resin using the His-Tag on the SNAP-25 molecule. TCEP was also removed during this purification step. Then the 2,260-bp DNA handle containing an activated thiol group at its 5' end was added to the solution of SNARE complex, with a SNARE complex to DNA handle molar ratio of 20:1 (*17, 21, 37*). Intramolecular and intermolecular crosslinking occurred in open air between the cysteine residues on syntaxin and VAMP2 and between VAMP2 and the DNA handle, respectively, in 100 mM phosphate buffer, 0.5 M NaCl, pH 8.5. The DNA handle also contains two digoxigenin moieties at another end. Both the thiol group and Digoxigenin moieties on the handle were introduced in the PCR reaction through PCR primers. The excess of SNARE complexes in the crosslinking mixture was removed after the SNARE complex-DNA conjugates were bound to the anti-digoxigenin coated beads.

High-resolution optical tweezers experiments

The dual-trap high-resolution optical tweezers were built, calibrated, and tuned to one base pair (0.34 nm) resolution, mainly as previously described (*17, 21, 38-40*). Data were acquired at 20 kHz, mean- filtered online to 10 kHz, and saved on a hard disk for further analysis. Experiments were carried out at room temperature (22 °C) in the PBS buffer (137 mM of NaCl, 2.7 mM of KCl, 8.1 mM of Na_2HPO_4, 1.8 mM of KH_2PO_4, pH 7.4), supplemented with oxygen scavenging system (*17, 21*). In the pulling-relaxation experiment, single SNARE complexes were pulled or relaxed by increasing or decreasing the separation between the two optical traps at the same speed of 10 nm/sec.

Data analysis

Force-extension models of the SNARE protein and the DNA handle. General methods used to fit the force-extension curves and to calculate the energy and kinetics at zero force have been described previously (*17, 21*), with a few modifications adapted for SNARE proteins. Briefly, the force-extension relationship of the unfolded polypeptide portion of the SNARE proteins and the DNA handle is described by the worm-like chain model. For the unfolded polypeptide, the model is described by the Marko-Siggia formula (*41, 42*)

$$F = \frac{k_B T}{P_m}\left[\frac{1}{4\left(1-\frac{x_m}{l}\right)^2}+\frac{x_m}{l}-\frac{1}{4}\right], \quad (1)$$

where F and x_m are the tension and extension of the polypeptide, respectively. Here $l = 0.365 \times N$ nm is the contour length of the polypeptide and related to the number of amino acids N in the polypeptide, assuming 0.365 nm contour length per amino acid (*13, 43*). The persistence length of polypeptide P_m is chosen as 0.6 nm for the energy and reaction rate calculations (*17, 21*). Finally, the constant $k_B T$ =4.1 pN×nm. Similarly, the Marko-Siggia formula for the DNA handle can be written as

$$F = \frac{k_B T}{P_{DNA}}\left[\frac{1}{4\left(1-\frac{x_{DNA}}{L_{DNA}}\right)^2}+\frac{x_{DNA}}{L_{DNA}}-\frac{1}{4}\right], \quad (2)$$

The measured extension of the protein-DNA tether (X) is

$$X = x_{DNA} + x_m + h, \quad (3)$$

where h is the state-dependent extension of the structured part of the SNARE complex (Fig. S10). X is the extension referred throughout this paper (such as those in the FEC plots). If the SNARE structure is completely unfolded, we set $h = 0$. If the SNARE structure is a helix bundle (either two-, three-, or four-helix bundle), the extension is not zero and dependent on the pulling direction relative to the helical axis of the bundle. If the SNARE structure is pulled perpendicular to the helical axis, $h = 2$ nm corresponding to the diameter of the coiled coil (*16*); If the structure is pulled in an axial direction, $h = 0.15 \times N_s$ nm where 0.15 nm is the helical rise per amino acid in an α-helix and N_s the number of amino acids in the helix.

The force and extension are related to the trap separation (D), the experimental control parameter, by the following equation:

$$\frac{F}{k_{trap}} + X + R_1 + R_2 = D, \tag{4}$$

where $k_{trap} = k_1 k_1 / (k_1 + k_2)$ is the effective force constant of the two optical traps with force constants k_1 and k_2, and R_1 and R_2 are the diameters of the beads in the two traps (*21*). The force (F), extension (X), trap separation (D), and other experimental parameters $(L_{DNA}, k_1, k_2, k_{trap}, R_1, R_2)$ can be obtained from tweezers experiments. Therefore, given the parameters corresponding to different SNARE structures, one can calculate their extension and tension by solving the system equations (1)-(4). The tension was computed as the root of the Matlab function tweezer_force_fun in Section *Matlab codes* in *Materials and Methods*.

Energy and kinetics of the dumbbell detection system. The folding and unfolding transitions of the SNARE protein observed in the dual-trap optical tweezers are coupled to optical traps and the DNA handle. Thus we need to consider the free energy function of the whole dumbbell detection system, which can be expressed as the sum of the energy of the optical traps, the protein complex, and the DNA handle, i.e.,

$$E(D,l) = \frac{F^2}{2k_{trap}} + E_m(l) + G(l) + E_{DNA}(F). \tag{5}$$

Here the total energy has been indicated as a function of the trap separation and the total contour length of the unfolded polypeptide pulled by optical traps (l). This contour length is chosen as a reaction coordinate to define the free energy of the folded portion of the SNARE protein $G(l)$ and of the corresponding unfolded portion. Thus, the total protein energy in the trap includes the folding free energy $G(l)$ and the entropic energy $E_m(l)$ of stretching the unfolded polypeptide portion of the protein to force F or extension x_m. Specifically, the entropic energy can be written as (*17*)

$$E_m(l) = \frac{k_B T}{P_m} \frac{l}{4\left(1 - \frac{x_m}{l}\right)} \left[3\left(\frac{x_m}{l}\right)^2 - 2\left(\frac{x_m}{l}\right)^3 \right]. \tag{6}$$

The entropic energy of the DNA handle $E_{DNA}(F)$ can be similarly expressed.

The energy function in Eq. (5) defines the energy landscape of SNARE folding/assembly in optical traps, given its energy landscape $G(l)$ at zero force. However, our purpose is to determine the latter from experimental measurements, including unfolding probability and transition rates. This inverse problem can be conveniently solved for some characteristic points in the energy landscape. For a two-state folding/unfolding process, suppose the free energy of the folded, unfolded, and transition states (if any) at zero force are $G_f, G_u,$ and $G^\dagger$, respectively. These states are located at $l_f, l_u,$ and $l^\dagger$ in the contour length reaction coordinate. Then their corresponding free energy in the presence of force can be calculated from Eq. (5), which are

denoted as E_f, E_u, and $E^\dagger$. For a downhill folding process at zero force, the transition state is not defined. However, a nominal transition state can be defined by the contour length $l^\dagger$ corresponding to the transition state in the presence of force. Then the unfolding probability is calculated as

$$p_u = \frac{e^{-E_u}}{e^{-E_f} + e^{-E_u}}. \tag{7}$$

Here we have chosen the energy unit as k_BT. Based upon Kramers' theory, the folding rate (k_f) and unfolding rate (k_u) can be written as

$$\begin{aligned} k_f &= k_m \exp\left(E_f - E^\dagger\right), \\ k_u &= k_m \exp\left(E_u - E^\dagger\right), \end{aligned} \tag{8}$$

respectively, where $k_m \approx 1\times10^6$ s^{-1} is the molecular transition rate representing the maximum protein folding rate (*44*). The unfolded state has a known contour length and its free energy at zero force is often chosen zero as an energy reference. To determine the energy and position of the folded state and the transition state ($G_f, G^\dagger, l_f, l^\dagger$), we fit the calculated opening probability, transition rates, average state forces, and/or extension changes to the corresponding experimental measurements and determine these parameters through nonlinear least-square fitting (*17, 21*). If the derived folding energy barrier $G^\dagger - G_u < 0$, the folding is called barrier-less and down-hill, as is shown for folding of the C-terminal SNARE domain here and other coiled coil proteins described elsewhere (*21*). The Matlab codes used for the fitting are listed in Section *Matlab codes* of *Materials and Methods*, including the main Matlab script (SNARE_energy_rate_fit.m) and six Matlab functions.

Force-extension curve (FEC) fitting. The extension of the SNARE complex in each state is calculated based on the model shown in fig. S10. The extension consists of the extension of the unfolded polypeptide $l_i r$ with contour length $l_i, i = 1,\cdots,5$ and the extension of the folded portion. The former can be calculated by the Marko-Siggia formula and the latter is assumed to be force-independent. The total protein-DNA tether extension X corresponding to the five states can be calculated as a function of force and contour lengths of the different states. Alternatively, we can simultaneously fit the extensions against the different regions of the measured FEC with the contour lengths as fitting parameters and determine their best-fit values. Note that the contour length for the fully unfolded state (or state 5) is known and not chosen as a fitting parameter ($l_5 = 68.3$ nm). The fitting is generally performed after the force and extension are mean-filtered to 91 Hz (or using a time window of 11 ms). The FECs are also shown in this bandwidth in the figures throughout the main and supplementary texts if not otherwise specified. To improve the fitting, the persistence lengths of the DNA and polypeptide are also chosen as fitting parameters in the regions of 30-50 nm and 0.5-0.6 nm, respectively. The fitting yields the averages of the best-fit contour lengths for different SNARE states $l_1 = 11$ (±1) nm, $l_2 = 19$ (±2) nm, $l_3 = 29$ (±2)

nm, $l_4 = 46$ (±1) nm. The Matlab function Marko_Siggia in the *Matlab codes* was used for the fitting.

Estimation of the total free energy from assembly of a single SNARE complex. This free energy is calculated as the sum of the folding free energy of three domains: LD (8 k_BT), CTD (28 k_BT) and NTD (35 k_BT), subtracted by the approximate coupling energy between NTD and CTD. This coupling energy has contributed to the measured folding energy of both CTD and NTD, thus it has been counted twice. Since t-SNARE is largely structured, this coupling energy is equivalent to the energy to initiate the coil-to-helix transition of the Vc domain. Based on the Zimm-Bragg model of the helix-to-coil transition (*45*), this initiation energy is about 6 k_BT (*46, 47*). Therefore, the energy of de novo NTD assembly is 29 k_BT. This coupling energy is important to understand SNARE assembly. For example, after t-SNARE is disassembled, the linker domains of syntaxin and VAMP2 become too weak to dimerize by themselves in the absence of CTD under our experimental conditions, even when the syntaxin and VAMP2 conjugate is relaxed to low forces (Fig. 2B & Fig. 3A). In contrast, LD can zipper against a high force (~12 pN) with an energy output of 8 k_BT, after CTD is already zippered. Thus, SNARE assembly is a team work of three SNARE domains.

Hidden-Markov modeling (HMM) analysis. The algorithms used for the HMM analysis have been described previously (*17, 48-51*). The two-state HMM analysis was performed on the time-dependent extension trace mean-filtered to 5 kHz. The idealized state transitions were also calculated at this frequency bandwidth and shown in Fig. 1D, which have higher temporal resolution than the extension traces shown at 556 Hz. It is worth clarifying the mean-filtering method used throughout our work. Suppose a time series $x_1, x_2, \cdots, x_N$ is defined on N time points with a uniform time interval Δt, i.e., $\Delta t, 2\Delta t, \cdots, N\Delta t$, then the mean-filtered time series X is defined as

$$X_j = \frac{1}{m} \sum_{k=(j-1)m+1}^{jm} x_k, \quad j = 1, 2, \cdots, N_X, \tag{9}$$

where N_X is the modulus of N versus the number of data points (m) chosen for the averaging. Correspondingly, these filtered data points are defined on the time points

$$T_j = mj\Delta t - (m-1)\Delta t / 2. \tag{10}$$

Thus the original time series x is filtered to X with a frequency bandwidth of $1/(m\Delta t)$. This mean-filtering method ensures that the detection noises in the extension traces, such as those from the Brownian motion of the beads, remain independent between different data points, a fundamental requirement for the HMM analysis (*48*). Other smoothing methods like the moving-box averaging may introduce correlation between neighboring data points. Such filtered data cannot be used for HMM analysis.

The filtered data were analyzed by the Matlab script idealize_general.m in *Matlab codes* to reveal average state positions, lifetimes, and unfolding equilibrium constants.

Comparison of the methods to measure the energy of SNARE assembly: SFA, AFM, and OT

The energetics and kinetics of SNARE assembly have been measured by a variety of biophysical approaches. These include spectroscopic methods based on CD and fluorescence detection (*10, 12, 15, 52*), isothermal titration calorimetry (ITC) (*28*), atomic force microscopy (AFM) (*30, 53-56*), and the surface forces apparatus (SFA) (*31*). These methods have defined the energy of SNARE assembly in the range of 20-35 k_BT, much lower than our measurement of 65 k_BT by optical tweezers (OT). The inconsistent energy measurement highlights many challenges in characterizing the energy and kinetics of SNARE assembly.

SFA

In the SFA experiment, t- and v-SNAREs were anchored on two supported lipid membranes on mica surfaces through the C-termini of syntaxin and VAMP2 (*31*). The SNAREs were brought close to form ternary complexes and then pulled apart to measure the rupture force. With a stiff force probe (>10^9 pN/nm), SFA is used to pull typically 10^5 SNARE complexes simultaneously (*31*). Based on the rupture force measured by SFA, SNARE assembly energy of 35±8 k_BT was obtained. For technical reasons, the two SNARE anchoring points could not be brought closer than ~4 nm. Compared to the results obtained from OT, this minimal separation prevents folding of the linker domain and part of the C-terminal SNARE domain of the complex. Therefore, SNARE disassembly observed by SFA corresponds to unzipping of the N-terminal region of SNARE. This leads to a smaller assembly energy derived from the SFA experiment than the energy (~ 65 k_BT) from the OT experiment.

AFM

AFM has been widely used to mechanically unfold single proteins, in particular SNARE complexes (*30, 53-56*). In this method, t- and v-SNAREs are often immobilized onto nickel-coated surfaces of the glass coverslip and of the cantilever tip through the C-terminal his-tags in syntaxin and VAMP2. Single SNARE complexes can be assembled in situ by bringing the tip and the glass surface close and then pulled by separating the glass surface from the tip. Thus mis-assembled SNARE complexes can be avoided, allowing functionally assembled complexes to be studied. In a typical force loading rate of 20 nN/s, the SNARE complex breaks in the force range of 100-500 pN, with a mean rupture force of 256 pN (*30*). The rupture occurs at an average extension of ~12 nm. This extension was interpreted as unfolding of the C-terminal SNARE domain to the ionic layer of the 4-helix bundle, with the assumption that the unzipped syntaxin and VAMP2 remained in an α-helical conformation with an extension of 0.15 per amino acid. However, this assumption was not justified due to the marginal stability of α-helices alone at room temperature (*17, 21, 57, 58*). Therefore, at least the unzipped VAMP2 region must be unfolded, with an extension of ~0.365 nm per amino acid. Therefore, only 9 or 6 amino acids in the C-terminal SNARE domain of VAMP2 was unzipped, assuming an intact or C-terminally unfolded t-SNARE complex, respectively, just before the rupture. This small Vc unzipping contrasts with 26 amino acids Vc unzipping measured from our OT experiment. Interestingly, this small unzipping corresponds to unfolding to the high local force region identified by us (Fig. 4).

AFM could only be applied to manipulate SNARE complexes in a high force region (>100 pN) (*30, 54*), due to its lower force resolution (~10 pN) (*59*) than OT (0.02 pN). Because many SNARE domains can only survive for a short time period under such a high tension, single complexes have to be pulled and characterized quickly in a dynamic manner. As a result, only the hard cores of the complex can be studied as described above. This explains why the distinct

linker domain and Vc domain transitions were not observed by AFM. More importantly, only SNARE disassembly was observed by AFM, because SNAREs cannot assembly in the high force range. Therefore, AFM-based experiments have not measured the energy of SNARE assembly so far (Fig. 4, the energy difference between states 1 and 4). What was derived from the AFM experiments was the activation energy of SNARE disassembly (23±8 k_BT) (*30*), approximately corresponding to the energy difference between state 2 and the energy barrier between states 3 and 4. Although this activation energy has not been fully characterized in our OT experiment, our energy model of SNARE assembly (Fig. 4) predicts an activation energy ≥ 57 k_BT for SNARE disassembly (from state 2 to state 4). Thus, our OT experiments yield a much greater lifetime of the SNARE complex (>1 billion years) than the AFM experiments (~2 seconds). The large difference in the activation energy or lifetime may be caused by the different energy barriers probed by AFM and OT. The AFM experiments were carried out under a condition that is far from equilibrium. As a result, the energy barrier identified in this case may not be well extrapolated to zero force and does not represent the dominant energy barrier for SNARE disassembly (*60, 61*).

Similarly, the AFM experiments derived activation free energy of 21±8 k_BT to mechanically unfold the binary complex between syntaxin and VAMP2 (*30*). This seemly high activation energy does not necessarily mean a high folding energy of the binary complex. Furthermore, to derive the activation energy, the authors adopted a pre-constant of K_a=3.3×10^9 s^{-1} in the Kramers rate equation that is much higher than the pre-constant of ~ 1×10^6 s^{-1} used in most protein or nucleic acid folding studies (*24, 44, 58, 62*), including our work. Using latter pre-constant, the activation energy is re-calculated as 13±8 k_BT. The folding energy of the binary complex is expected to be much lower than this energy.

OT

Optical tweezers are well-suited to the study of intermediate states in protein folding processes (*13, 43*) and have been successfully applied to two-stranded leucine zipper proteins (*17, 21, 58*). Two small polystyrene or silica beads are tightly and specifically attached to different sites of a single macromolecule. Light is used to hold one bead in place while forcing the other to move, thereby applying a known mean force across the trapped protein molecule, and separation of the beads is continuously monitored. When sufficient force is applied to cause a portion of the protein to cooperatively unravel, a jump in separation occurs whose size reveals a folding unit within the protein. At a critical force, the unit may spontaneously flicker between compact (folded) and extended (unfolded) states due to thermal fluctuations, revealing both the energetics and the kinetics of the transitions (*17, 22*).

Both OT and AFM have been widely used to manipulate single molecules and measure the force and extension responses to their structural transitions in real time. Optical tweezers appear to show higher resolution than AFM in protein folding studies and have clearly shown reversible unfolding and refolding transitions of many proteins (*13, 43, 58, 59, 63-65*). OT have large dynamic ranges of measurements, e.g., 0.02-200 pN in force, 0.2-10^5 nm in distance and 1x10^{-4}-3x10^3 s in time (*38, 39*). This makes it possible to accurately characterize the multiscale folding kinetics of proteins from a single experiment on a single molecule (*17, 21*). The high resolution of OT results from the low stiffness and the small size of their force probes (beads in optical traps) and the differential detection (*39*). Therefore, one can apply very accurate forces to detect the reversible unfolding and refolding transitions, identify the SNARE assembly intermediates, and measure the energy change association with each transition or intermediate in equilibrium.

Such equilibrium transitions occur at a low force range (< 20 pN) and cannot be detected by AFM with a force resolution of greater than 10 pN.

Besides higher resolution of OT, our OT experiments improve the experimental setup compared to AFM and SFA experiments. First, the SNARE complexes are crosslinked at either N- or C-termini of syntaxin and VAMP2, which allows dynamic SNARE disassembly and reassembly not possible in the previous experiments. Second, the SNARE complexes are pulled via a long DNA handle, instead of directly attaching SNARE complexes to two surfaces. The use of the DNA handle avoids the nonspecific interactions common in single-molecule manipulation experiments (*13*, *65*, *66*). It also minimizes the steric effects to facilitate force and extension detection. Finally, the syntaxin molecule used in our experiment lacks its N-terminal H_{abc} domain, compared to the full cytoplasmic syntaxin used in the AFM and SFA experiments. The presence of this N-terminal domain may hinder SNARE assembly and reduce the energy of SNARE zippering (*9*, *67*).

Due to these improvements based on OT, we have obtained several new findings. We have identified two discrete intermediates in SNARE assembly (states 2 and 3), quantified their associated energy and transition kinetics using an equilibrium method, and measured the full assembly energy of cytoplasmic SNAREs (~65 k_BT) much higher than previous measurements (20-35 k_BT). We have also shown that the half-zippered intermediate (3) only exists in a high force load (12 pN <F< 20 pN) and can fold at diffusion-limited rate. The strong force-dependence of the state has likely made it elusive in previous experiments. Although atomic force microscopy and the surface forces apparatus (SFA) can apply forces to SNARE complexes (*30*, *31*), they lack sufficient force resolution to stabilize the partially zippered state in the narrow force range. The half-zippered intermediate (3) temporally separates the slow NTD association and fast CTD and LD zippering, indicating its important role in the calcium-triggered synaptic vesicle fusion.

The two intermediates observed in our OT experiments are significantly different in structure and foldability from any partial SNARE structures derived from AFM and SFA. We have demonstrated that these intermediates are energetic and their further zippering can serve as the power stroke for membrane fusion. In contrast, the corresponding C-terminal regions (especially the linker domain) of the partial SNARE structures are too weak to be detected by AFM and SFA. Thus, results from both approaches did not distinguish the following two scenarios: (i) whether these regions are disordered or structured in solution, and (ii) whether these partial structures represent a spectrum of intermediates during progressive SNARE zippering or discrete intermediates for binary switching clearly seen in our OT experiments.

Matlab codes

To run the following Matlab codes, we recommend that the codes be copied and saved into different files in the same folder. The names of Matlab functions are highlighted in bold. Matlab Optimization Toolbox is required.

1. **Unfolding probability, transition rate, and extension fitting (SNARE_energy_rate_fit.m)**

```
% This program fits trap-separation dependent opening probability (two-state
% process),unfolding rate, folding rate, folded state force, and unfolded
% state force, and/or state position difference

% Data to be fitted. In order of trap separation, unfolding prob,
% unfolding rate, folding rate, folded state force, unfolded state force,
% and extension change(optional)
filename='InputData.dat';

ktrap=0.06; % Effective trap stiffness
% Parameters in the model
L_DNA=2260*0.34;  % DNA length in nm
p_DNA=40; % DNA persistence in nm
% p_DNA=51.5/(1+2.78*51.5/L_DNA);
p_m=0.6;  % Persistence length of polypeptide in nm
kmax=1e6; % Maximum transition rate
Lmax=28.5; % Contour length of the unfolded state

% Read experimental data
fname=filename(1:length(filename)-4);
a=textread(filename);
[nd,nc]=size(a);
D0=a(:,1);  % Trap separation
ydata0=a(:,2:6); % Data to be fit

% The thermodynamic average force
fav=ydata0(:,4)+(ydata0(:,5)-ydata0(:,4)).*ydata0(:,1);

ydata0(:,2:3)=log(ydata0(:,2:3));  % Use logarithm rate for fitting
ymin=min(ydata0);
ymax=max(ydata0);

[nr,nc]=size(ydata0);

% Use the scaled data or weighted data for fitting
scale=ones(nr,nc); % Weight chosen to be one in this case

xdata=D0;  % Convert to one-column array
ydata=ydata0;
ydata=ydata.*scale;
mask=isnan(ydata);
% Account for the missing data points (indicated by Nan in the data file)
```

```
ydata(mask)=0;

% Calculate the intial bead diameters
[Dmax,ind]=max(xdata); % Maximum trap separtion
fmax=ydata(ind,5); % The force corresponding to the maximum trap separtion
% R_init is the intial bead diameter
R_init=Dmax-fmax./ktrap-L_DNA.*Marko_Siggia(fmax,p_DNA)-
Lmax.*Marko_Siggia(fmax,p_m);

% Initial fitting parameters
x0=[20.2    23.2    -30     -11     -39  ];
lb=[18.8     11     -40     -40     -100 ];
ub=[20.2    28.5    -20     10      100  ];
Ls=[2,2,2]; % Coiled coil diameters

options = optimset('PlotFcns',@optimplotresnorm,'TolFun',1e-6);
% Define the fitting function
f=@(x,xd)tweezer_fun_SNARE_noext(x,xd,scale,mask,Lmax,p_m,L_DNA,p_DNA,...
kmax,ktrap,Ls);
% The main fitting function
[x,resnorm] = lsqcurvefit(f,x0,xdata,ydata,lb,ub,options);

% Calculate critical trap separation and force
Vm=[x(3) x(4) 0];
Lm=[x(1) x(2) Lmax];
R=x(5);

Ls_corr=zeros(size(Lm)); % add alpha-helical length in the pulling direction
alpha=0.15/0.365;
Ls_corr=Ls+(Lm-Lm(1)).*alpha;

% Define function of the unfolding probability
p=@(y)tweezer_pop(y,R,ktrap,Vm,Lm,p_m,L_DNA,p_DNA,kmax,Ls_corr);

D_start=mean(D0);
[Dc,value]=fzero(p,D_start); % Dc is the calculated critical trap separation

% Calculate the critical state forces, rates, and other parameters
[fc,extc,energyc,popc,ratec,fluc_c]=tweezer_measure(Dc,R,ktrap,Vm,Lm,...
p_m,L_DNA,p_DNA,kmax,Ls_corr);

% Calculate the energy of different components in the system
kT=4.1;
[rd,kd,ed]=Marko_Siggia(fc,p_DNA); % DNA handle
[rm,km,em]=Marko_Siggia(fc,p_m); % Unfolded polypeptide
etrap=fc.*fc./ktrap./2./kT; % Trap
eDNA=L_DNA.*ed./kT;  % Energy of the DNA handle
em=[Lm(1) Lm(3)].*em./kT;  % Energy of the polypeptide (Eq. 6).
emi=[Vm(1) Vm(3)];  % Folding energy of the protein
disp([etrap' eDNA' em' emi']);
energy=etrap+eDNA+em+emi; % Total system energy corresponding to Eq. (5)
disp(energy)

fh=mean(fc);   % Equilibrium force
rateh=mean(ratec); % Equilibrium transition rate
```

```
dexth=diff(extc);  % The calculated extension change

% Fitting the experimental data
yfit=f(x,xdata);
yfit=yfit./scale;
yfit(mask)=NaN;

yfit0=yfit;

ydata0(:,2:3)=exp(ydata0(:,2:3));  % convert back to rates
yfit0(:,2:3)=exp(yfit0(:,2:3));

% Calculate actual middle force
fmfit=mean(yfit0(:,4:5)');
fmfit=fmfit';

% Linear regression between middle force and trap separation
fm=(mean(ydata0(:,4:5)'))';
p=polyfit(a(:,1),fm,1);
fmid=polyval(p,a(:,1)); % The middle force

hut=figure('name','Unfolding prob vs Trap separation');
plot(D0,ydata0(:,1),'*k',D0,yfit0(:,1),'o-r')
xlabel('Trap separation (nm)')
ylabel('Unfolding prob.')
saveas(hut,[fname '_unfold_trapsep.fig'])

huf=figure('name','Unfolding prob vs force');
plot(fmid,ydata0(:,1),'*k',fmid,yfit0(:,1),'o-r')
xlabel('Force (pN)')
ylabel('Unfolding prob.')
saveas(huf,[fname '_unfold_f.fig'])

hrt=figure('name','Rates vs Trap separation');
semilogy(D0,ydata0(:,2:3),'*k',D0,yfit0(:,2:3),'o-r');
xlabel('Trap separation (nm)')
ylabel('Rate (1/s)')
saveas(hrt,[fname '_rate_trapsep.fig'])

hrf=figure('name','Rates vs force');
semilogy(fmid,ydata0(:,2:3),'*k',fmid,yfit0(:,2:3),'o-r');
xlabel('Force (pN)')
ylabel('Rate (1/s)')
saveas(hrf,[fname '_rate_f.fig'])

hft=figure('name','Force vs Trap separation');
plot(D0,ydata0(:,4:5),'*k',D0,yfit0(:,4:5),'o-r');
xlabel('Trap separation (nm)')
ylabel('Force (pN)')
saveas(hft,[fname '_f_trapsep.fig'])

disp(['file name:' , filename])
disp(['p_DNA= ' num2str(p_DNA,3) ' p_m= ' num2str(p_m)])
disp(xan)
disp('Lower and upper bounds :')
```

```
disp([lb; ub])
disp('Best-estimated parameters:')
disp(x)
disp('Fitting error: ')
disp(resnorm)
disp('Critical trap separation, force, extension difference, and rate')
format short g
disp([Dc fh dexth rateh])

file_out=[fname '_out.mat'];
save file_out


function Fun=tweezer_fun_SNARE_noext(x,D,scale,mask,Lmax,p_m,L_DNA,p_DNA,
kmax,ktrap,Ls)
%  Function for non-linear least sqare fitting
%  x: fitting parameter array
%  D: 1D array of trap separation
%  scale: The scaling factor (or weight) for experimental data fitting
%
    n=length(x);
    nL=3;
    nst=2;  % Number of states
    Lm=zeros(1,nL);  % extension of state and barrier
    Vm=zeros(1,nL);  % The corresponding energy
    Lm(1:nL-1)=x(1:nL-1);
    Lm(nL)=Lmax;  % Contour length of the fully unfolded state
    Vm(1:nL-1)=x(nL:2*(nL-1));
    Vm(nL)=0;  % Assume the completely unfolded state having zero energy
    R=x(5);  % Total bead radius

    Ls_corr=zeros(1,nL); % add alpha-helical length in the pulling direction
    alpha=0.15/0.365;
    Ls_corr=Ls+(Lm-Lm(1)).*alpha; % Extension of the folded portion

    [force,ext,energy,pop,rate,fluc]=tweezer_measure(D,R,ktrap1,Vm,Lm,p_m,
     L_DNA,p_DNA,kmax,Ls_corr);

    Fun=[pop(:,2) log(rate) force];
    % ext(:,2)-ext(:,1)
    Fun=Fun.*scale;
    Fun(mask)=0;

end

function punfold=tweezer_pop(D0,R,ktrap,Vm,Lm,p_m,L_DNA,p_DNA,kmax,Ls)
%  Function used to calculate the trap separation at which a two-state
%  system has half unfolding probability
    M=length(Lm);
    nst=(M+1)/2;  % Number of states
    nb=M-nst;  % Number of energy barrier
    ext=zeros(1,nst);
    force=zeros(1,nst);
    fluc=zeros(1,nst);
    pop=zeros(1,nst);
```

```
    energy=zeros(1,M);
    nrate=2*nb;
    rate=zeros(1,nrate);
    f_start=16;


[force,ext,energy,pop,rate,fluc]=tweezer_measure(D0,R,ktrap,Vm,Lm,p_m,L_DNA,
 p_DNA,kmax,Ls);

    punfold=pop(nst)-0.5;

end



function [force,ext,energy,pop,rate,fluc]=tweezer_measure(D,R,ktrap,Vm,Lm,
p_m,L_DNA,p_DNA,kmax,Ls)
% This function calculates the average force, extension, energy, population,
% associated rates and fluctuations of different states,  given related
% parameters used for experiments on the dual-trap optical tweezers.
% The units used are pN for force, nm for length, and pNxnm for energy
% Output:  force: state force
%          ext: state extension
%          energy: energy of state and barrier
%          pop: state population
%          rate: transition rate
%          fluc: state fluctuation
% Input:   D: The separation between the two traps
%          R: Sum of the diameters of the two beads
%             ktrap: Effective stiffness of the two traps (k1*k2/(k1+k2)).
%          Vm: array of energy defining the energy landscape of the
%              molecule
%          Lm: Contour length of the molecule defing the states and energy
%              barriers. Its length has to be odd
%          p_m: Persistence length of the molecule of interest
%          L_DNA: Contour length of the total DNA handle length
%          p_DNI: Persistence length of the DNA handle
%          kmax: Molecular transition rate
%          Ls: Extension of the structured portion of the molecule

    kT=4.1;
    N=length(D); % Number of trap separation tested
    M=length(Lm); % Number of characteristic points in energy landscape
    nst=(M+1)/2;  % Number of states. Valid only for 1-D energy landscape
    nb=M-nst;  % Number of energy barrier
    ext=zeros(N,nst);  % state extension at different trap separation
    force=zeros(N,nst);  % state force
    fluc=zeros(N,nst);  % state fluctuation
    pop=zeros(N,nst);  % state population
    energy=zeros(N,M); % state energy and barrier
    nrate=2*nb;     % Number of reaction rates
    rate=zeros(N,nrate);
    f_start=20;  % Initial value for equilibrium force calculation.
    f0=zeros(N,M); % Average force corresponding to state and barrier

    for i=1:N  % Different trap separation
```

```
        for j=1:M % Different contour length
            % Calculate the equilibrium force at different trap separation
            % (i) and % contour length (j)
            fun=@(x)tweezer_force_fun(x,D(i),R,ktrap,Lm(j),
                 p_m,L_DNA,p_DNA,Ls(j));
            [f,value]=fzero(fun,f_start);
            if(abs(value)>1e-5)
                disp('Root not found')
                format short g
                a=[D(i),R,ktrap,Lm(j),p_m,L_DNA,p_DNA];
                disp(a)
                disp('force= ')
                disp([f value])
                format
            end
            f0(i,j)=f;
        end
        % Calculate extension, force constant, and energy per unit
        % contour length for DNA and polypeptide
        [rd,kd,ed]=Marko_Siggia(f0(i,:),p_DNA); % DNA handle
        [rm,km,em]=Marko_Siggia(f0(i,:),p_m); % Polypeptide
        % Total elastic energy
        energy(i,:)=f0(i,:).*f0(i,:)./ktrap./2+L_DNA.*ed+Lm.*em;
        % Convert to kT. Total system energy
        energy(i,:)=energy(i,:)./kT+Vm;
        % Unfolding rate
        rate(i,1:2:nrate)=kmax.*exp(energy(i,1:2:M-1)-energy(i,2:2:M));
        % Folding rate
        rate(i,2:2:nrate)=kmax.*exp(energy(i,3:2:M)-energy(i,2:2:M));
        % State extension
        ext(i,:)=L_DNA.*rd(1:2:M)+Lm(1:2:M).*rm(1:2:M)+R+Ls(1:2:M);
        % State force
        force(i,:)=f0(i,1:2:M);
        energy_cor(i,:)=energy(i,:)-mean(energy(i,:));  % Avoid over-flow
        % State population
        pop(i,:)=exp(-energy_cor(i,1:2:M))./sum(exp(-energy_cor(i,1:2:M)));
        % Total compliance of DNA and polypeptide
        ct=L_DNA./kd(1:2:M)+Lm(1:2:M)./km(1:2:M);
        kt=1./ct+ktrap; % Effective force constant
        fluc(i,:)=sqrt(kT./kt); % State fluctuation
    end
end


function y=tweezer_force_fun(f,D,R,ktrap,L_m,p_m,L_DNA,p_DNA,L0)
   % f: force
   % D: Trap separation
   % R: =r1+r2: total bead diameter
   % ktrap: k1*k2/(k1+k2) overal trap stiffness
   % L_m, p_m: The contour length and persistence of the molecule of
   %           interest
   % L_DNA, p_DNA: The contour length and persistence of DNA.
   % L0: Extension of the structured portion
   y=f./ktrap+L_DNA.*Marko_Siggia(f,p_DNA)+L_m.*Marko_Siggia(f,p_m)+L0+R-D;
end
```

```
function [ratio kms energy]=Marko_Siggia(f,P)
% Calculate the extension, force constant, and energy density of a
% worm-like chain using the Marko-Siggia formula
% Input:
%          f: force (pN)
%          P: persistence length (nm)
% Output:
%          ratio: the ratio of extension to contour length (x/L)
%          kms: force constant (pN/nN) per unit contour length. The actual
%               force constant for the chain is kms/L where L is the
%               contour length.
%          energy: elastic energy per unit contour length (pN.nm)

   n=length(f);
   if(n>1)
       ratio=zeros(size(f));
       for i=1:n
           ratio(i)=ext_force_formula1(f(i),P);
       end
   else
       ratio=ext_force_formula1(f,P);
   end
   if(nargout>=2)
      kms=4.1./P*(1+0.5.*(1-ratio).^-3);
   end
   if(nargout>=3)
       energy=4.1./P./4./(1-ratio).*ratio.*ratio.*(3-2.*ratio);
   end
end



function ext=ext_force_formula1(f,P)
% This function calculate the DNA extension when a pulling force is
% supplied, using Marko-Siggia formula. Note that the ext output is the ratio
% of DNA extension to DNA contour length.

r_start=1-0.5*sqrt(4.1/P/f);
if(r_start<0.2)
    r_start=0.1;
end

fun=inline('4.1./P.*(0.25./(1-x)^2+x-0.25)-f','x','P','f');
ff=@(x)fun(x,P,f);
[ext,value]=fzero(ff,r_start);
if(abs(value)>1e-6)
    disp('Root not found')
    disp(value)
end
```

2. HMM analysis (idealize_general.m)

```
% This program requires the Hidden Markov Model toolbox to perform the HMM
% analysis. The toolbox was written by Kevin Murphy and can be downloaded
% from http://www.cs.ubc.ca/~murphyk/Software/HMM/hmm.html.
% For an introduction to HMM, please refer to
% L. R. Rabiner, A tutorial on hidden Markov-models and selected applications
% in speech recognition. Proc. IEEE. 77, 257 (1989).

clear all
close all

% Read time-extension data into variable a,supposing the first column is
% time,
% and the second column the extension
a=load('SampleTraceforHMM.txt');

% Plot the time-extension trace
figure
plot(a(:,1),a(:,2))
x=a(:,1)';
obs=a(:,2)';

T=length(obs); % Number of data points
Q=2; % Number of states

% Setting the initial parameters for HMM analysis. These parameters should
% be adjusted based on the input data
initial_prob0 = [1 0]';  % the probability being in state 1 at time zero
transmat0 = [0.99 0.01; 0.01 0.99]; % The transition probability matrix
mu0=[4440 4460]; % Initial state position in extension
Sigma0=25.*ones(1,1,Q); % State fluctuation
mixmat0=ones(Q,1);

% Optimizing HMM parameters using E-M algorithm
[LL, prior1, transmat1, mu1, Sigma1, mixmat1] = ...
    mhmm_em(obs, initial_prob0, transmat0, mu0, Sigma0, mixmat0,'thresh',
            1e-6, 'max_iter', 60,'adj_mix',0);

% Calculate the maximum likehood
loglik = mhmm_logprob(obs, prior1, transmat1, mu1, Sigma1, mixmat1);

mu1 % The optimized state position

transmat1 % The optimaized transition probability matrix

keq_sim=transmat1(1,2)/transmat1(2,1) % Equilibrium constant

sqrt(Sigma1) % Optimal state fluctuation

% State idealization
obslik = mixgauss_prob(obs, mu1, Sigma1);
path = viterbi_path(prior1, transmat1, obslik); % The idealized states
obs_id=mu1(1)+(mu1(2)-mu1(1)).*(path-1); % Convert to idealized extension
```

```
% Plot the input and idealized time-extension traces
figure
plot(x,obs,'-k',x,obs_id,'+r')
```

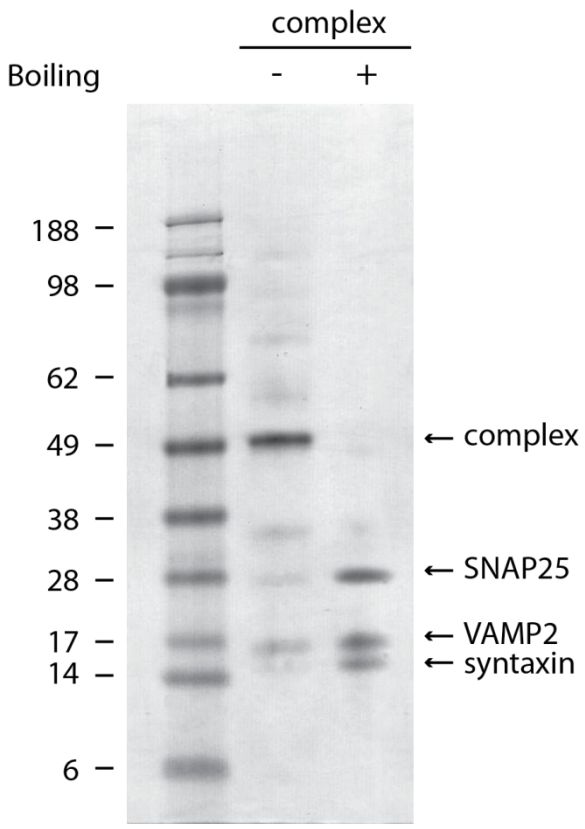

Fig. S1. Characterization of the ternary SNARE complex based on its SDS resistance. The SNARE complex is resistant to SDS, but dissociates when boiled to 100 °C. The SNARE proteins were assayed by 12% SDS gel electrophoresis. Left lane, the protein ladder with protein masses shown on the left. Middle lane, the ternary SNARE complex purified by gel filtration. Right lane, the same SNARE complex boiled to 100 ˚C for 10 min prior to loading on the gel. Identities of the different protein bands are labeled on the right.

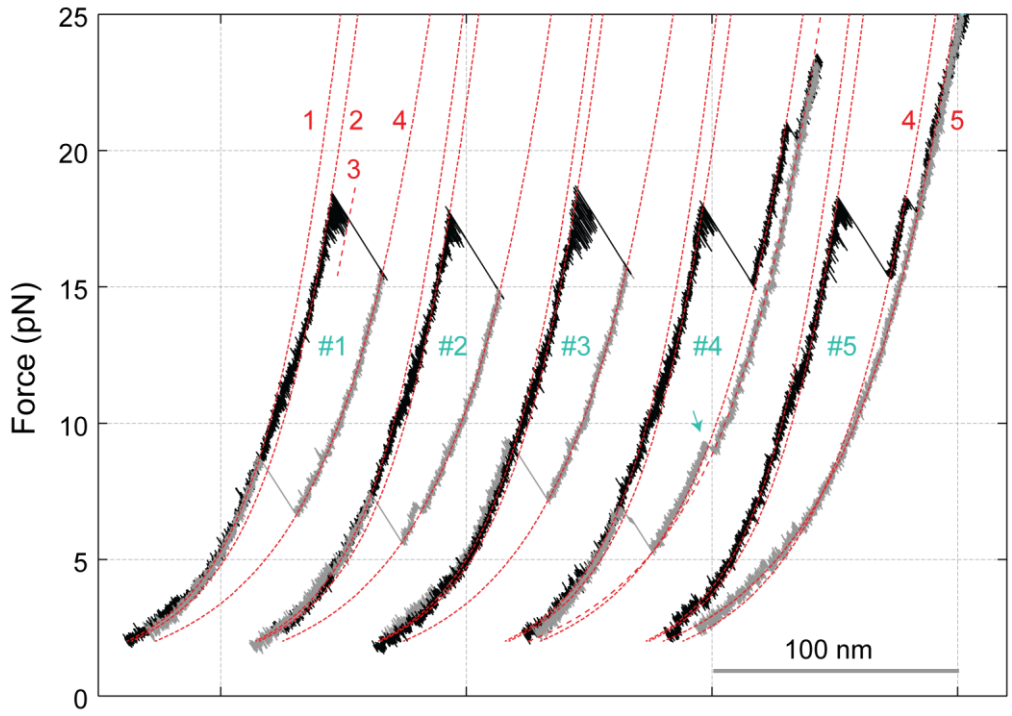

Fig. S2. Force-extension curves (FECs) obtained by repeatedly pulling (black) and relaxing (gray) a single SNARE complex for five rounds. Note that the extensions in this and other FEC plots throughout this paper have been shift along the x axis for clarity. The FECs are split into at least five distinct regions by two reversible and at least three irreversible extension or force transitions, indicating five different SNARE assembly states. The best fits of the different regions of the FECs are shown as red dashed lines. After t-SNARE was unfolded (FEC #4), a small percentage (overall ~15 %) of the syntaxin and VAMP2 conjugate could reassemble into the ternary SNARE complex upon relaxation to low forces. The reassembly was always followed by a refolding event at a higher force (marked by the cyan arrow), indicating t-SNARE formation. This t-SNARE reassembly was probably induced by the SNAP-25 molecule nonspecifically associated with the syntaxin molecule or bound back before it diffused away under our experimental conditions, even after the t-SNARE had been disrupted by force. The force and extension here are shown at 200 Hz, as well as those in Fig. 1B. Note that the overall extension increase due to SNARE unzipping is not significantly greater than the axial length of the SNARE complex (Fig. 1A), due to compliance of the DNA handle and the unfolded polypeptide and the force drop accompanying each SNARE unfolding event. See *Materials and Methods* and Ref. (*17*).

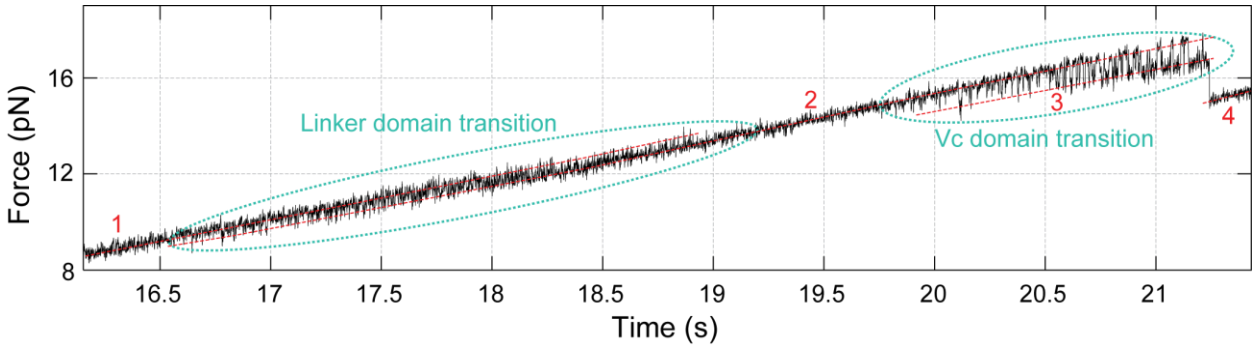

Fig. S3. Time-dependent instantaneous force corresponding to the extension shown in Fig. 1C when the SNARE complex was being pulled at a trap separation speed of 10 nm/sec. Reversible folding/unfolding transitions of the linker domain and the Vc domain are marked in dashed and solid ovals, respectively. Different states involved in the transitions are numbered in red as in Fig. 1. Consistent with Fig. 1C, data are shown at 1000 Hz.

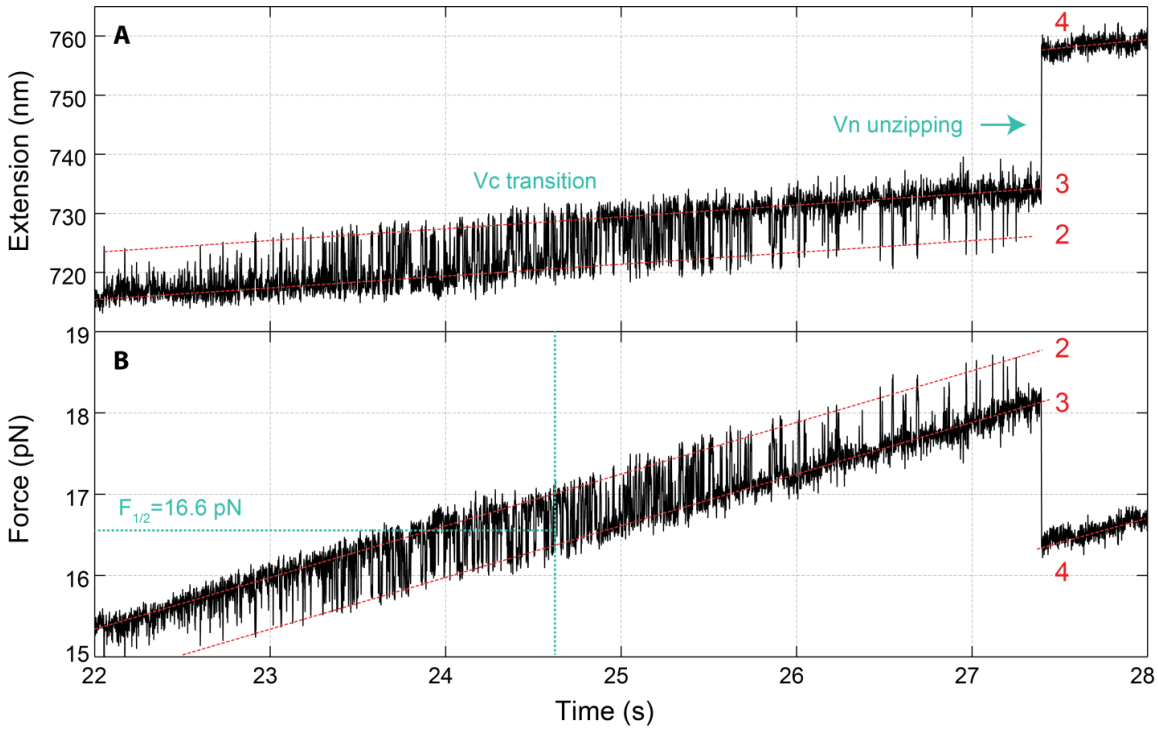

Fig. S4. Reversible zippering and unzipping of the C-terminal SNARE domain of VAMP2 (Vc) on the t-SNARE complex. (**A**) Time-dependent extension as the SNARE complex is being pulled by increasing the trap separation at a speed of 10 nm/sec. Note that the Vc domain gradually shifts to the partially unzipped state with greater average extension (state 3) during the pulling process. The jump at the end of the trace indicates abrupt unzipping of the N-terminal domain of VAMP2 (Vn) from the t-SNARE complex. (**B**) Time-dependent instantaneous force corresponding to the extension in **A**. The equilibrium unzipping force is the average force corresponding to equal populations of the zippered and unzipped states. Traces shown here are mean-filtered to 1000 Hz.

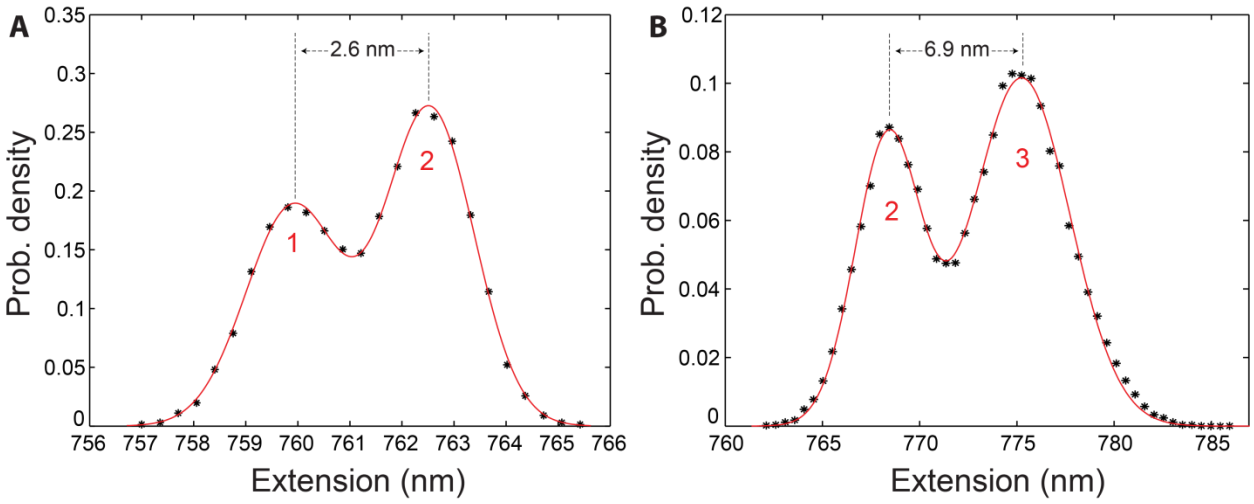

Fig. S5. Histogram distributions of extension (symbols) and their double-Gaussian function fitting (red lines) showing reversible transitions in the linker domain (**A**) and the Vc domain (**B**). The corresponding extension traces are shown in Fig. 1D. The average extension changes in the transitions are indicated. Note that the histogram distributions were calculated when the extension traces were filtered to different bandwidths, 556 Hz for the linker domain (A) and 5 kHz for the Vc domain (B).

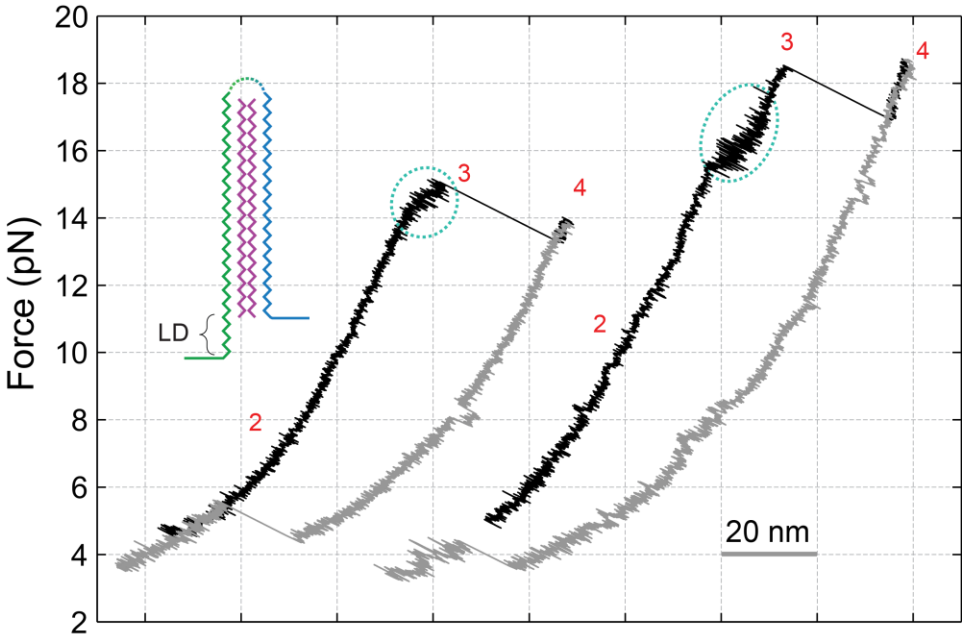

Fig. S6. Force-extension curves of the SNARE complexes lacking the linker domain in VAMP2 (Inset). Compared to FECs with the intact linker domain shown in Fig. S2, the transition at 8-13 pN disappears, whereas the Vc domain transition remains (regions in green ovals). The conclusion is supported by inspection of 46 FECs at 2000 Hz temporal resolution in which no linker domain transition is found. Except for the linker domain transition, the FECs for this complex are similar to that of the SNARE complex with intact linker domains.

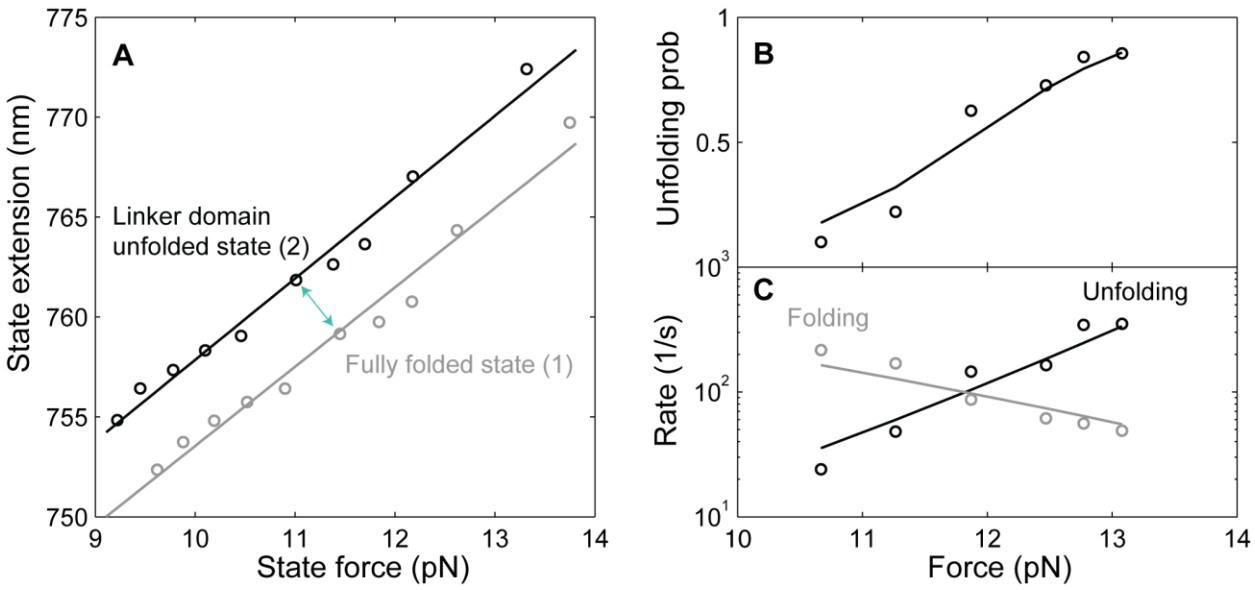

Fig. S7. Representative extension, energy, and kinetics of the linker domain measured from a single SNARE complex. (**A**) Average state extensions as a function of average forces for the linker domain folded state (gray circle) and the unfolded state (black circle). The average state extension and force are determined by the HMM analysis. The linear fit of the extension is shown as the line. Note that the observed state transition occurs between different state forces, as indicated by the dashed arrows. (**B**) Probability being in the unfolded state as a function of the mean force (symbols) and its best fit (line). (**C**) Force-dependent folding and unfolding rates and their best theoretical fit. The theoretical fit of the unfolding probability and rates are calculated as described in *Materials and Methods*.

The average contour length change ($\Delta l = l_2 - l_1$, see Fig. S10) involved in the transition can be calculated as follows: First, the best-fits of the extension for the folded and unfolded states corresponding each state force value (F_i) are calculated. The extension-to-contour length ratio (r_i) is computed using the Marko-Siggia formula, i.e.,

$$F_i = \frac{k_B T}{P_m}\left[\frac{1}{4(1-r_i)^2} + r_i - \frac{1}{4}\right]. \tag{11}$$

Then the contour length difference at this force point is evaluated based on the model shown in Fig. S10 as

$$\Delta l_i = \Delta x_i / r_i \tag{12}$$

where Δx_i is the extension difference between the two states now under the same tension F_i. Finally, the average of these contour length differences is calculated. The average contour length difference involved in the linker domain transition calculated from the experiment on this SNARE complex is 7.9 (±0.2) nm, or 21.6 (±0.5) amino acids.

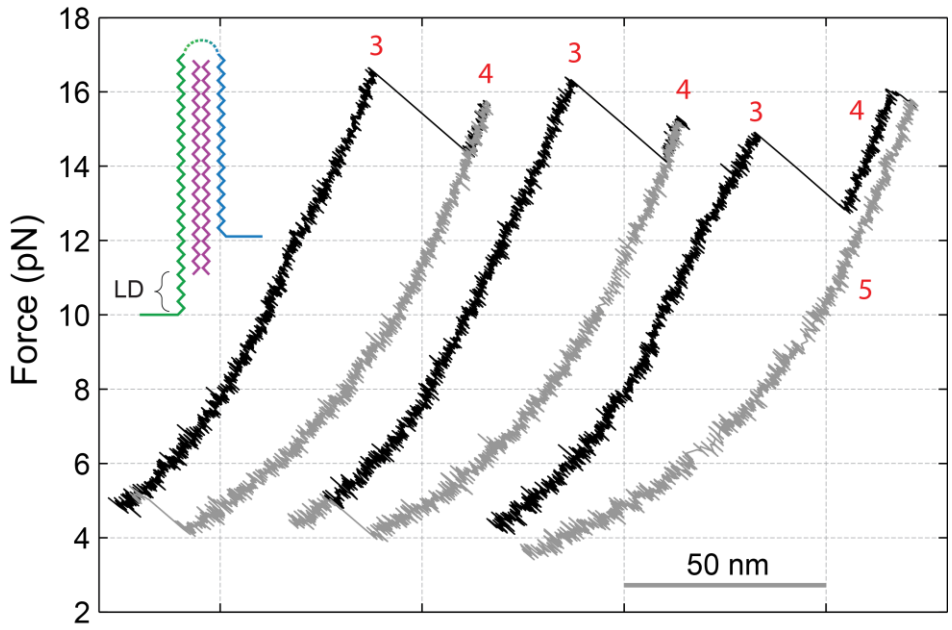

Fig. S8. Force-extension curves of the SNARE complexes lacking the linker domain and part of the Vc domain in VAMP2 (Inset). Note that the reversible transition just before the first unfolding jump (from states 3 to 4) disappears for these SNARE complexes, a finding supported by 51 FECs inspected at 2000 Hz bandwidth compared to 91 Hz bandwidth shown here. Compared with the FECs with both domains (Fig. S2) and with the Vc domain alone (Fig. S6), we conclude that the Vc domain contributes to the folding and unfolding transition at 15-19 pN before Vn domain is unzipped. In this experiment only part of the Vc domain is deleted, the remaining part of the Vc domain unzips continuously before the Vn domain is unzipped. This observation is consistent with a high energy density at the C-terminal end of CTD (Fig. 4).

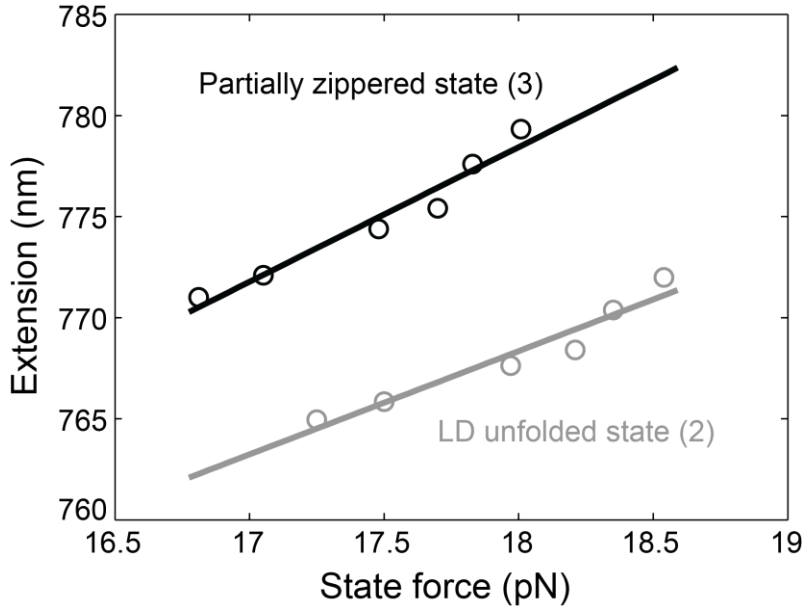

Fig. S9. Representative average state extensions as a function of average state forces for the Vc-domain folded (gray circle) and unfolded states (black circle) from a single SNARE complex and the linear fit of the extensions (lines). The average contour length change involved in the Vc domain transition is calculated as described in the legend of Fig. S7, except that Eq. (12) is replaced by

$$\Delta l_i = \Delta x_i / \left(r_i + \alpha \right) \tag{13}$$

to account for the extension contribution of the folded t-SNARE structure based on the model shown in Fig. S10. The average contour length change measured from this experiment is 9.0 (±0.7) nm, or 25 (±2) amino acids.

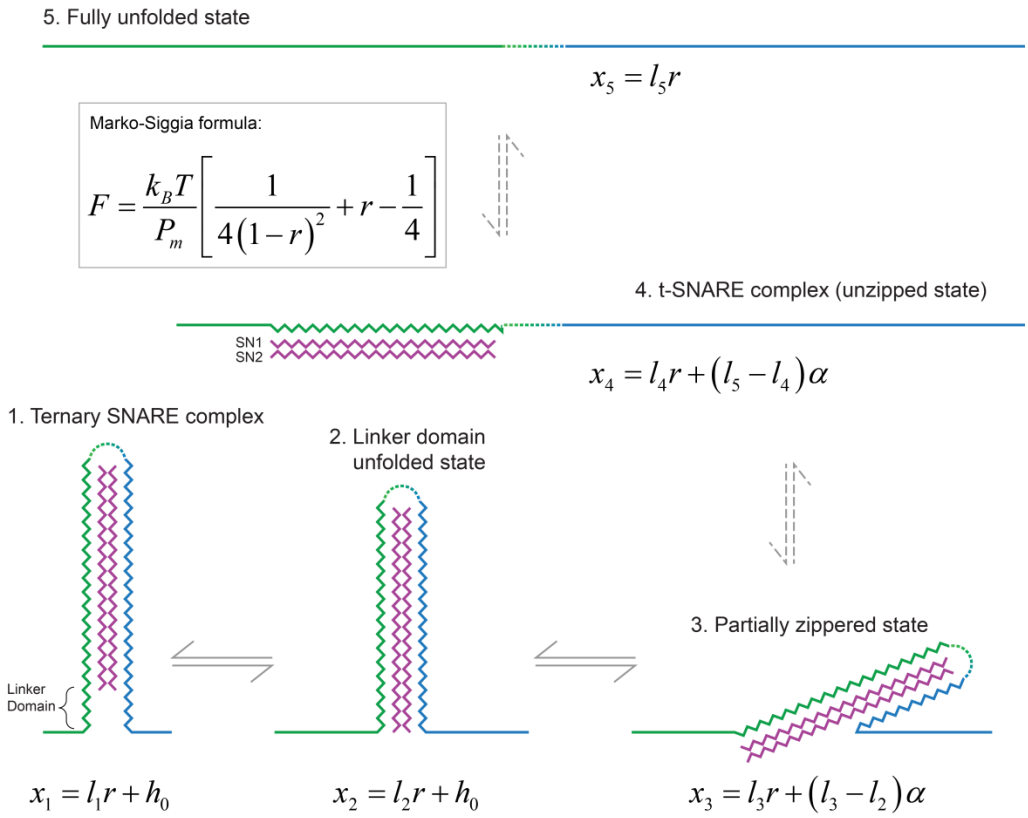

Fig. S10. Schematic model of the extension changes of the SNARE complex in its different assembly states. Here $l_i, i = 1,\cdots,5$ is the contour length of the unfolded polypeptide in different SNARE assembly states, h_0 =2 nm the diameter of the coiled coil, and $\alpha = 0.15/0.365 = 0.41$ the ratio of the contour length of an amino acid in the helical conformation to that in the coil conformation. The extension of the unfolded polypeptide is related to the contour length and force through the Marko-Siggia formula shown (*41*). Note that the linker domain is symmetrically zippered and unzipped between states 1 and 2, because individual α-helices only have marginal stability in solution and cannot resist the observed high forces involved in the transition (*17*). In contrast, the Vc domain asymmetrically transits between states 2 and 3, in which the t-SNARE remains mainly structured when the Vc domain is being pulled out. Finally, we found that the syntaxin molecule is approximately fully α-helical (61 a.a.) in the t-SNARE complex through FEC fitting (*Materials and Methods*). This implies that one or two of the SNARE domains in SNAP-25 (SN1 and SN2) are associated with the syntaxin molecule to keep syntaxin in an α-helical conformation. However, we favor the three-helix bundle conformation for the t-SNARE complex observed in our experiments, because only a three-helix bundle can resist the high tension in the range of 15-28 pN under which the t-SNARE complex is first generated. This tension range is well above the equilibrium force of the two-stranded GCN4 coiled coil subject to an axial pull (~ 12 pN) (*17*). Thus the three-helix bundle shown in state 4 is more likely to be the structure of the t-SNARE complex.

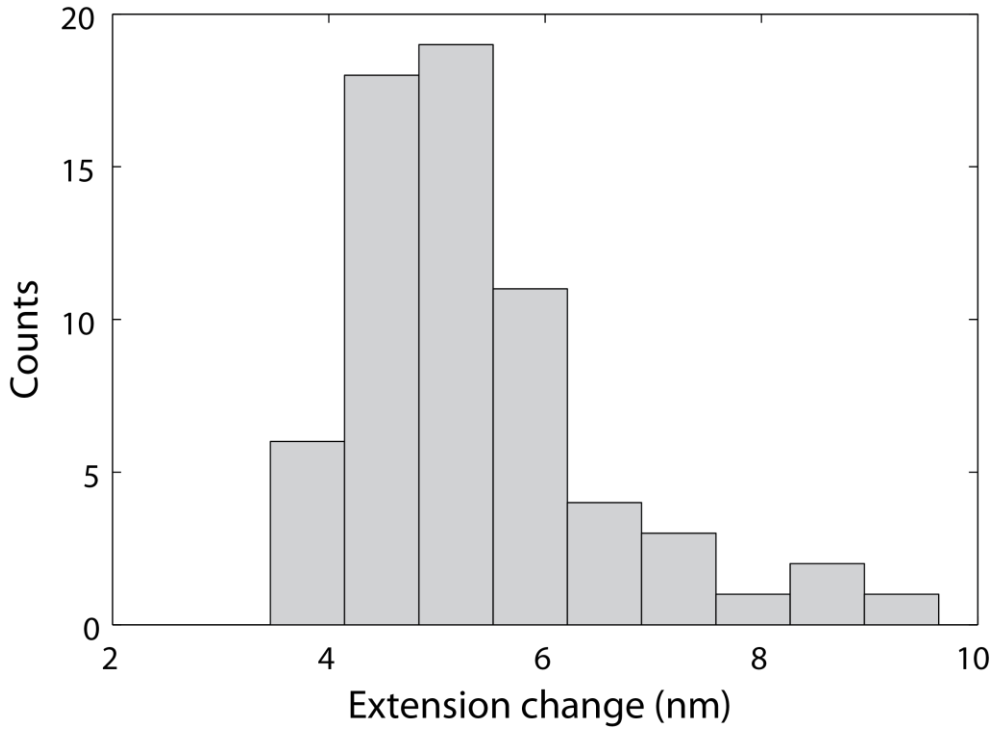

Fig. S11. Histogram distribution of the extension increase upon t-SNARE unfolding. A total of 65 t-SNARE unfolding events obtained from pulling the ternary SNARE complexes at both C-termini (Fig. 1) and N-termini (Fig. 3) were pooled to calculate the histogram distribution. The average extension change is 5.3 nm, with a standard deviation of 1.2 nm. The t-SNARE complex unfolds at a force range between 13 pN and 28 pN, partially contributing to the observed variation in the extension change shown in the distribution, due to the compliance of the DNA handle and the unfolded portion of the polypeptide (*17*, *68*).

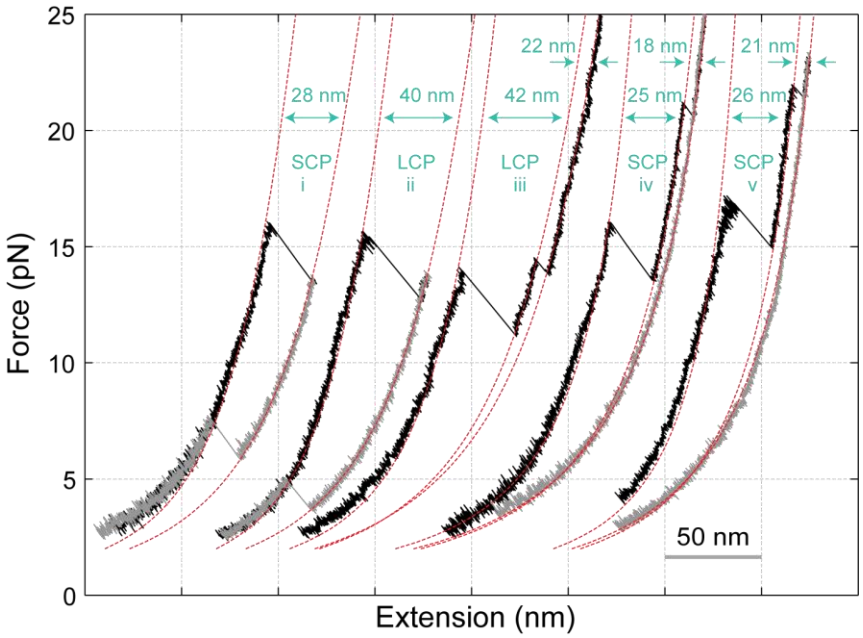

Fig. S12. Comparison of the FECs for two sets of SNARE complexes with short (SCP) and long (LCP) N-terminal loops between syntaxin and VAMP2. LCP has 36 more amino acids in the loop than SCP, based upon the prediction of the crystal structures of SNARE complexes (*4*, *16*). This leads to greater average contour length release of LCP (41 nm) than that of SCP (26 nm) when the SNARE complex completely unzips its N-terminal domain. The contour lengths of the unfolded polypeptide in different SNARE states are determined by fitting the corresponding FEC regions using the structural model shown in Fig. S10 and methods described in *Materials and Methods*. The best-fit curves in these regions are shown in red lines. The contour length differences between the corresponding states (indicated by green numbers) reveal that LCP has 39 (±5) more amino acids in the loop region than SCP, consistent with the sequence extension. Another difference between the two constructs is that LCP reassembles at lower force than SCP (Table S1). The long loop in LCP makes it kinetically unfavorable for zippering between t- and v-SNAREs.

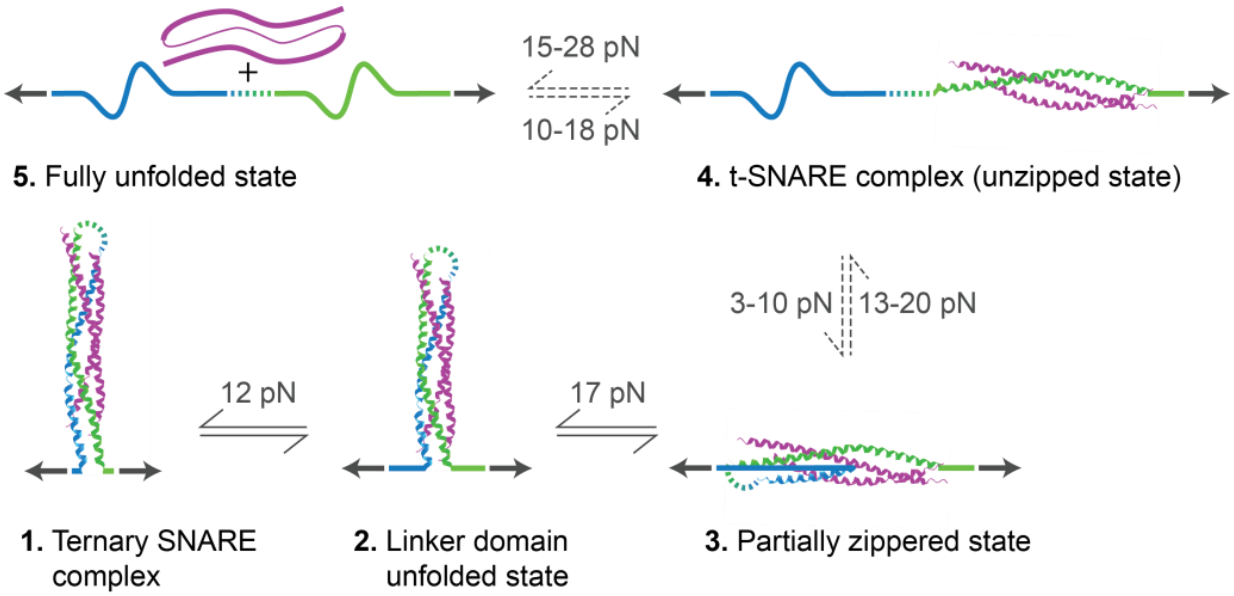

Fig. S13. Intermediates and pathways of SNARE assembly and disassembly. The equilibrium and non-equilibrium transitions are indicated by solid and dashed arrows, respectively, along with their equilibrium forces or force ranges labeled.

SNARE constructs	Linker domain		Vc domain		Vn domain		t-SNARE disassembly		SNARE assembly	
	Size (nm)	Force (pN)	Size (nm)	Force (pN)	Size (nm)	Force (pN)	Size (nm)	Force (pN)	Size (nm)	Force (pN)
SCP	2.9 (0.5)	11.7 (1.7)	7.1 (1.0)	16.7 (1.6)	14.6 (1.4)	16.7 (1.5)	5.1 (1.0)	18.3 (3.6)	-11.1 (2.8)	5.0 (1.0)
LCP	3.1 (0.7)	11.5 (1.6)	7.4 (1.3)	16.1 (1.8)	22.5 (1.8)	16.4 (1.2)	5.7 (1.3)	17.0 (1.5)	-8.8 (1.2)	3.5 (0.3)
NP	N.A.	N.A.	13.5 (1.0)	17.8 (1.7)	8.3 (0.9)	18.5 (1.5)	5.4 (1.3)	18.4 (1.8)	-7.8 (1.9)	3.2 (0.9)

Table S1. Extension changes and forces accompanying structural transitions of different SNARE domains. The numbers in cyan represent parameters for equilibrium transitions, in which equilibrium forces and sizes of the average extension changes at the equilibrium forces are given. The numbers in black indicate parameters in non-equilibrium transitions, in which the size is the average extension change and the average force where the transition begins. The numbers in parentheses are the corresponding standard deviations. SCP, the SNARE complex with a short N-terminal loop for C-terminal pulling; LCP, the SNARE complex with a long N-terminal loop for C-terminal pulling; NP, the SNARE complex for N-terminal pulling. See *Materials and Methods* for details of these constructs.

References and Notes

1. T. Sollner *et al.*, SNAP receptors implicated in vesicle targeting and fusion. *Nature* **362**, 318 (1993).

2. T. Weber *et al.*, SNAREpins: Minimal machinery for membrane fusion. *Cell* **92**, 759 (1998).

3. T. C. Sudhof, J. E. Rothman, Membrane fusion: Grappling with SNARE and SM proteins. *Science* **323**, 474 (2009).

4. R. B. Sutton, D. Fasshauer, R. Jahn, A. T. Brunger, Crystal structure of a SNARE complex involved in synaptic exocytosis at 2.4 angstrom resolution. *Nature* **395**, 347 (1998).

5. P. I. Hanson, R. Roth, H. Morisaki, R. Jahn, J. E. Heuser, Structure and conformational changes in NSF and its membrane receptor complexes visualized by quick-freeze/deep-etch electron microscopy. *Cell* **90**, 523 (1997).

6. F. S. Cohen, G. B. Melikyan, The energetics of membrane fusion from binding, through hemifusion, pore formation, and pore enlargement. *J. Membr. Biol.* **199**, 1 (2004).

7. T. Xu *et al.*, Inhibition of SNARE complex assembly differentially affects kinetic components of exocytosis. *Cell* **99**, 713 (1999).

8. S. Y. Hua, M. P. Charlton, Activity-dependent changes in partial VAMP complexes during neurotransmitter release. *Nat. Neurosci.* **2**, 1078 (1999).

9. T. J. Melia *et al.*, Regulation of membrane fusion by the membrane-proximal coil of the t-SNARE during zippering of SNAREpins. *J. Cell Biol.* **158**, 929 (2002).

10. A. V. Pobbati, A. Stein, D. Fasshauer, N- to C-terminal SNARE complex assembly promotes rapid membrane fusion. *Science* **313**, 673 (2006).

11. A. M. Walter, K. Wiederhold, D. Bruns, D. Fasshauer, J. B. Sorensen, Synaptobrevin N-terminally bound to syntaxin-SNAP-25 defines the primed vesicle state in regulated exocytosis. *J. Cell Biol.* **188**, 401 (2010).

12. M. Kyoung *et al.*, In vitro system capable of differentiating fast Ca2+-triggered content mixing from lipid exchange for mechanistic studies of neurotransmitter release. *Proc. Natl. Acad. Sci. U.S.A.* **108**, E304 (2011).

13. C. Cecconi, E. A. Shank, C. Bustamante, S. Marqusee, Direct observation of the three-state folding of a single protein molecule. *Science* **309**, 2057 (2005).

14. Materials and Methods in the Supplementary Materials.

15. K. Weninger, M. E. Bowen, S. Chu, A. T. Brunger, Single-molecule studies of SNARE complex assembly reveal parallel and antiparallel configurations. *Proc. Natl. Acad. Sci. U.S.A.* **100**, 14800 (2003).

16. A. Stein, G. Weber, M. C. Wahl, R. Jahn, Helical extension of the neuronal SNARE complex into the membrane. *Nature* **460**, 525 (2009).

17. Y. Gao, G. Sirinakis, Y. L. Zhang, Highly anisotropic stability and folding kinetics of a single coiled coil protein under mechanical tension. *J. Am. Chem. Soc.* **133**, 12749 (2011).

18. D. Kummel *et al.*, Complexin cross-links prefusion SNAREs into a zigzag array. *Nat Struct Mol Biol* **18**, 927 (2011).

19. D. Fasshauer, R. B. Sutton, A. T. Brunger, R. Jahn, Conserved structural features of the synaptic fusion complex: SNARE proteins reclassified as Q- and R-SNAREs. *Proc. Natl. Acad. Sci. U.S.A.* **95**, 15781 (1998).

20. F. Li *et al.*, Complexin activates and clamps SNAREpins by a common mechanism involving an intermediate energetic state. *Nat Struct Mol Biol* **18**, 941 (2011).

21. Z. Q. Xi, Y. Gao, G. Sirinakis, H. L. Guo, Y. L. Zhang, Direct observation of helix staggering, sliding, and coiled coil misfolding. *Proc. Natl. Acad. Sci. U.S.A.* **109**, 5711 (2012).

22. M. T. Woodside *et al.*, Direct measurement of the full, sequence-dependent folding landscape of a nucleic acid. *Science* **314**, 1001 (2006).

23. B. L. Sabatini, W. G. Regehr, Timing of neurotransmission at fast synapses in the mammalian brain. *Nature* **384**, 170 (1996).

24. J. Kubelka, J. Hofrichter, W. A. Eaton, The protein folding 'speed limit'. *Curr. Opin. Struct. Biol.* **14**, 76 (2004).

25. J. F. Ellena *et al.*, Dynamic structure of lipid-bound synaptobrevin suggests a nucleation-propagation mechanism for trans-SNARE complex formation. *Proc. Natl. Acad. Sci. U.S.A.* **106**, 20306 (2009).

26. Y. Xu, L. J. Su, J. Rizo, Binding of Munc18-1 to synaptobrevin and to the SNARE four-helix bundle. *Biochemistry-Us* **49**, 1568 (2010).

27. E. Karatekin *et al.*, A fast, single-vesicle fusion assay mimics physiological SNARE requirements. *Proc. Natl. Acad. Sci. U.S.A.* **107**, 3517 (2010).

28. K. Wiederhold, D. Fasshauer, Is assembly of the snare complex enough to fuel membrane fusion? *J. Biol. Chem.* **284**, 13143 (2009).

29. K. Weninger, M. E. Bowen, U. B. Choi, S. Chu, A. T. Brunger, Accessory proteins stabilize the acceptor complex for synaptobrevin, the 1 : 1 syntaxin/SNAP-25 complex. *Structure* **16**, 308 (2008).

30. W. Liu, V. Montana, V. Parpura, U. Mohideen, Single molecule measurements of interaction free energies between the proteins within binary and ternary SNARE complexes. *J Nanoneurosci* **1**, 120 (2009).

31. F. Li *et al.*, Energetics and dynamics of SNAREpin folding across lipid bilayers. *Nat. Struct. Mol. Biol.* **14**, 890 (2007).

32. L. Shi *et al.*, SNARE proteins: one to fuse and three to keep the nascent fusion pore open. *Science* **335**, 1355 (2012).

33. W. S. Trimble, D. M. Cowan, R. H. Scheller, VAMP-1 - a synaptic vesicle-associated integral membrane-protein. *Proc. Natl. Acad. Sci. U.S.A.* **85**, 4538 (1988).

34. M. K. Bennett, N. Calakos, R. H. Scheller, Syntaxin - a synaptic protein implicated in docking of synaptic vesicles at presynaptic active zones. *Science* **257**, 255 (1992).

35. G. A. Oyler *et al.*, The identification of a novel synaptosomal-associated protein, SNAP-25, differentially expressed by neuronal subpopulations. *J. Cell Biol.* **109**, 3039 (1989).

36. I. S. Carrico, B. L. Carlson, C. R. Bertozzi, Introducing genetically encoded aldehydes into proteins. *Nat. Chem. Biol.* **3**, 321 (2007).

37. C. Cecconi, E. A. Shank, F. W. Dahlquist, S. Marqusee, C. Bustamante, Protein-DNA chimeras for single molecule mechanical folding studies with the optical tweezers. *Eur. Biophys. J.* **37**, 729 (2008).

38. E. A. Abbondanzieri, W. J. Greenleaf, J. W. Shaevitz, R. Landick, S. M. Block, Direct observation of base-pair stepping by RNA polymerase. *Nature* **438**, 460 (2005).

39. J. R. Moffitt, Y. R. Chemla, D. Izhaky, C. Bustamante, Differential detection of dual traps improves the spatial resolution of optical tweezers. *Proc. Natl. Acad. Sci. U.S.A.* **103**, 9006 (2006).

40. G. Sirinakis *et al.*, The RSC chromatin remodeling ATPase translocates DNA with high force and small step size. *EMBO J.* **30**, 2364 (2011).

41. J. F. Marko, E. D. Siggia, Stretching DNA. *Macromolecules* **28**, 8759 (1995).

42. C. Bustamante, J. F. Marko, E. D. Siggia, S. Smith, Entropic Elasticity of Lambda-Phage DNA. *Science* **265**, 1599 (1994).

43. J. Stigler, F. Ziegler, A. Gieseke, J. C. M. Gebhardt, M. Rief, The complex folding network of single calmodulin molecules. *Science* **334**, 512 (2011).

44. W. Y. Yang, M. Gruebele, Folding at the speed limit. *Nature* **423**, 193 (2003).

45. B. H. Zimm, J. K. Bragg, Theory of the phase transition between helix and random coil in polypeptide chains. *J Chem Phys* **31**, 526 (1959).

46. C. L. Brooks, Helix-coil kinetics: Folding time scales for helical peptides from a sequential kinetic model. *J Phys Chem-Us* **100**, 2546 (1996).

47. M. B. Jackson, SNARE complex zipping as a driving force in the dilation of proteinaceous fusion pores. *J. Membr. Biol.* **235**, 89 (2010).

48. L. R. Rabiner, A tutorial on hidden Markov-models and selected applications in speech recognition. *Proc. IEEE.* **77**, 257 (1989).

49. S. A. McKinney, C. Joo, T. Ha, Analysis of single-molecule FRET trajectories using hidden Markov modeling. *Biophys. J.* **91**, 1941 (2006).

50. S. Syed, F. E. Mullner, P. R. Selvin, F. J. Sigworth, Improved hidden Markov models for molecular motors. Part 1: Basic theory. *Biophys. J.* **99**, 3684 (2010).

51. F. Qin, A. Auerbach, F. Sachs, A direct optimization approach to hidden Markov modeling for single channel kinetics. *Biophys. J.* **79**, 1915 (2000).

52. D. Fasshauer, W. Antonin, V. Subramaniam, R. Jahn, SNARE assembly and disassembly exhibit a pronounced hysteresis. *Nat. Struct. Biol.* **9**, 144 (2002).

53. A. Yersin *et al.*, Interactions between synaptic vesicle fusion proteins explored by atomic force microscopy. *Proc. Natl. Acad. Sci. U.S.A.* **100**, 8736 (2003).

54. W. Liu, V. Montana, J. H. Bai, E. R. Chapman, V. Parpura, Single molecule mechanical probing of the SNARE protein interactions. *Biophys. J.* **91**, 744 (2006).

55. V. Parpura, U. Mohideen, Molecular form follows function: (un)snaring the SNAREs. *Trends Neurosci.* **31**, 435 (2008).

56. M. H. Abdulreda *et al.*, Pulling force generated by interacting SNAREs facilitates membrane hemifusion. *Integr Biol* **1**, 301 (2009).

57. S. Marqusee, R. L. Baldwin, Helix stabilization by Glu- ... Lys+ salt bridges in short peptides of de novo design. *Proc. Natl. Acad. Sci. U.S.A.* **84**, 8898 (1987).

58. J. C. M. Gebhardt, T. Bornschlogla, M. Rief, Full distance-resolved folding energy landscape of one single protein molecule. *Proc. Natl. Acad. Sci. U.S.A.* **107**, 2013 (2010).

59. K. C. Neuman, A. Nagy, Single-molecule force spectroscopy: optical tweezers, magnetic tweezers and atomic force microscopy. *Nat. Methods* **5**, 491 (2008).

60. S. B. Fowler *et al.*, Mechanical unfolding of a titin Ig domain: Structure of unfolding intermediate revealed by combining AFM, molecular dynamics simulations, NMR and protein engineering. *J. Mol. Biol.* **322**, 841 (2002).

61. P. M. Williams *et al.*, Hidden complexity in the mechanical properties of titin. *Nature* **422**, 446 (2003).

62. M. T. Woodside *et al.*, Nanomechanical measurements of the sequence-dependent folding landscapes of single nucleic acid hairpins. *Proc. Natl. Acad. Sci. U.S.A.* **103**, 6190 (2006).

63. J. P. Junker, F. Ziegler, M. Rief, Ligand-dependent equilibrium fluctuations of single Calmodulin molecules. *Science* **323**, 633 (2009).

64. T. Bornschlog, M. Rief, Single-molecule dynamics of mechanical coiled-coil unzipping. *Langmuir* **24**, 1338 (2008).

65. T. Bornschlogl, M. Rief, Single molecule unzipping of coiled coils: Sequence resolved stability profiles. *Phys. Rev. Lett.* **96**, (2006).

66. E. Celik, V. T. Moy, Nonspecific interactions in AFM force spectroscopy measurements. *J Mol Recognit* **25**, 53 (2012).

67. F. Parlati *et al.*, Rapid and efficient fusion of phospholipid vesicles by the alpha-helical core of a SNARE complex in the absence of an N-terminal regulatory domain. *Proc. Natl. Acad. Sci. U.S.A.* **96**, 12565 (1999).

68. W. J. Greenleaf, M. T. Woodside, E. A. Abbondanzieri, S. M. Block, Passive all-optical force clamp for high-resolution laser trapping. *Phys. Rev. Lett.* **95**, 2081021 (2005).